ADVANCED MATERIALS INTERFACES
Open Access
www.advmatinterfaces.de

Mechano-Bactericidal Activities of Orthopedic Implants with Nanostructured Surfaces: Recent Advances and Prospects

Yuzheng Wu, Pei Liu, and Paul K. Chu**

Orthopedic surgery enables patients to regain the functions of lost or damaged bone tissues, but success is often compromised by highly prevalent surgery site infections (SSIs). To prevent SSIs and avoid superbugs, mechano-bactericidal strategies are being developed to inactivate bacteria on nanostructured surfaces based on contact killing. The antibacterial mechanism of nanostructured surfaces stems from the physical force exerted on the bacterial membrane while imposing lower lethality on host cells. Owing to the bactericidal ability and biocompatibility, mechano-bactericidal approaches have become desirable in designing antibacterial surfaces for orthopedic implants. In this review, the latest advances in mechano-bactericidal strategies are described by discussing three commercial orthopedic materials approved by the United States Food and Drug Administration: titanium, magnesium, and polyether-ether-ketone. The recent developments and requirements of these three types of biomaterials are presented, and the feasibility and future directions of mechano-bactericidal surfaces are discussed.

1. Introduction

Orthopedic surgery is quite common nowadays as it improves the quality of life of many patients. It plays a vital role in repairing and restoring musculoskeletal functions and addressing bone defects. However, the prevalence of surgical site infections (SSIs) remains a significant challenge following orthopedic surgery. In certain surgical sites related to bone trauma, the incidence of SSIs can be as high as 50%.[1] The consequences of SSIs, including prolonged hospitalization, inflammation response,[2] additional surgeries, and antibiotic treatments, inevitably increase the trauma and financial burden of patients. While systemic administration of antibiotics serves as empirical prophylaxis and treatment for SSIs,[3] indiscriminate killing by antibiotics can damage the commensal microbiota in the body[4] and furthermore, the emergence of superbugs diminishes the effectiveness of therapies.[5] Hence, in order to enhance the surgical success and combat antimicrobial resistance (AMR), it is imperative to develop antibiotic-free strategies for the treatment and prevention of orthopedic SSIs.[6]

On the heels of the rapid development of materials and biological science, physical approaches have been used in bactericidal applications.[7] Among them, the mechano-bactericidal strategy is considered a potential alternative to antibiotic treatments and a useful tool to combat antibiotic-resistant bacteria because the antibacterial mechanisms are different from that of antibiotics. Unlike the chemical reaction rendered by antibiotics and ions, external mechanical stress provided by nanostructures is the key to bacterial elimination. As shown in **Scheme 1**, the antibacterial effects of mechano-bactericidal methods arise from membrane stretching between two nanopillars or membrane cutting by the sharp edges of nanosheets,[8] consequently producing membrane damage and rupture. Inspired by the scientific curiosity of natural products, the mechano-bactericidal effect was first discovered on the nanopillars of cicada wings.[9] Rapid bacterial killing is one characteristic of the mechanical strategy, with the bacterial inactivated within 6 min after attaching to the nanostructured surface.[10] Spurred by the recent development of nanotechnology, various nanostructures have been found to exhibit similar inhibition toward pathogens, including nanorods,[11] nanocolumns,[12] nanowires,[13] nanosheets,[14] nanospinules,[15] nanospikes, and nanocone arrays.[16] These nanostructures are usually exploited to mimic natural structures on the surface of bulk materials to foster contact-killing effects against bacteria.

Mechano-bactericidal strategies show great potential, especially for surface modification of orthopedic implants, because implant-related infections commence with bacterial adhesion on the biomaterials.[17] If the pathogens can be killed as they contact the surface, biofilm formation can be circumvented and infection will not occur. More importantly, eukaryotic cells have stronger tolerance on nanostructured surfaces. For example, according to Ivanova et al., fibroblast-like cells (COS-7) cover the nanopillars

Y. Wu, P. Liu, P. K. Chu
Department of Physics
Department of Materials Science and Engineering, and Department of Biomedical Engineering
City University of Hong Kong
Tat Chee Avenue, Kowloon, Hong Kong 518057, China
E-mail: pliu34-c@my.cityu.edu.hk; paul.chu@cityu.edu.hk

The ORCID identification number(s) for the author(s) of this article can be found under https://doi.org/10.1002/admi.202400004

DOI: 10.1002/admi.202400004

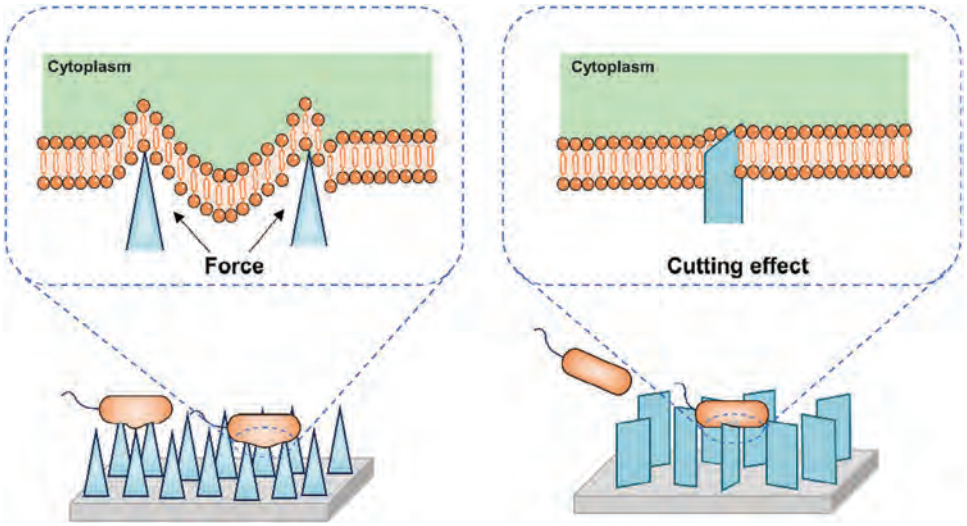

Scheme 1. Schematic diagram showing the membrane stretching and cutting effects on mechano-bacterial surfaces.

instead of the cell wall being punctuated in contrast to pathogenic bacteria.[18] Moreover, mechano-bactericidal orthopedic implants are non-leaching and local-serving, thus avoiding systemic toxicity. Owing to the good bactericidal activity and biosafety, nanostructured surfaces have a large potential in preventing orthopedic SSIs. In this review, the application of mechano-bactericidal methods to the surface modification of three types of orthopedic biomaterials approved by the United States Food and Drug Administration (US FDA), namely titanium (Ti) alloys, magnesium (Mg) alloys, and polyether-ether-ketone (PEEK), is described. The latest advances and potential development directions of the mechano-bactericidal strategy are also discussed.

2. Ti-Based Biomaterials and Implants

Since the 1940s, Ti-based implants have been used in orthopedics because of their lightweight, low elastic modulus, non-magnetism, non-toxicity, corrosion resistance, high strength, and good toughness.[19] The US FDA-approved Ti-based orthopedic implants include cranial mesh and craniofacial meshes (Meticuly Co, Ltd, Thailand),[20] talus spacers (Paragon 28 Inc., US), sacroiliac joint fusion devices (SI-BONE, US),[21] interbody fusion devices (Osseus Fusion Systems, US), etc.[22] As Ti lacks antibacterial ability, various strategies have been studied to endow Ti with antimicrobial properties, of which the mechano-bactericidal surface is one of the hot research topics. Both pure Ti and Ti-based alloys are used as substrates to construct nanostructured surfaces for orthopedic implants and the representative works are summarized in **Table 1**. The composition of the nanostructures can be classified into self-producing Ti-based materials and exogenous compounds. The former makes use of Ti in the substrate to generate nanostructures, whereas the latter relies on other elements to produce the nanostructures. In this section, mechano-bactericidal Ti surfaces are discussed according to the composition of the nanostructures, and the synergetic strategies to improve the antibacterial activity on nanostructured Ti surfaces are described.

2.1. Ti-Based Nanostructures

Nanostructures can be fabricated on Ti-based implants by extracting Ti from the substrate to form oxide and nitride. Among them, Ti oxide is widely studied, and hydrothermal (HT) methods are the most common. In the HT treatment, a TiO_2 layer is first formed on the substrate, and Ti^{4+} is dissolved from the TiO_2 precursor for the recrystallization of Ti compounds.[25,41] Through the dissolution and growth competition, various nanostructures can be fabricated, for example, spike-, sheet-, rod-, and wire-like surfaces. Nevertheless, orthopedic implants require not only bactericidal properties, but also biosafety and osteogenesis. Therefore, the influence of the nanotopography on host cells must be evaluated. Tristan et al. have compared the antibacterial ability, cytocompatibility, and osteogenesis properties of two different nanostructured surfaces (**Figure 1a**).[25] Plasma etching produces a Ti surface with a two-tier hierarchical topography on the microscale to reduce bacterial attachment and result in rupturing all the bacteria cell walls in contact with the surface (Figure 1b). However, an elevated β-galactosidase level is detected from human adipose-derived stem cells (hASCs) after culturing on this two-tier structure (Figure 1c), indicating accelerated cellular senescence. In contrast, a random nanostructured surface with sharp nanosheet protrusions prepared by HT etching cuts through the bacterial cell membranes to kill them without cellular senescence. Meanwhile, the growth, proliferation, and osteoinductive properties of hASCs are facilitated on the HT nanosheet surface without using external promotion and agents (Figure 1d), boding well for orthopedic applications. Hence, the nanopatterns for orthopedic implants must be tailored in order that the host cells are not damaged by the mechano-bactericidal surfaces while the antibacterial effects are retained.

While nanotextured surfaces are developed, the cause of bacterial death is also studied. In general, membrane damage produced by the sharp nanostructures leads to cytoplasm leakage and eventually inactivates the bacteria. In addition, the oxidation stress caused by the nano-morphology can reduce bacterial viability. Jenkins et al. have used TEM, FIB-SEM, and electron

Table 1. Representative mechano-bactericidal surfaces on Ti-based implants.

Substrates	Surface patterns	Preparation	Bacteria	Refs.
Ti	TiO_2 nanospikes	Hydrothermal (HT) synthesis	*E. coli* and *S. aureus*	[23]
Ti	TiO_2 nanospikes	Alkaline HT treatment	*E. coli* and *S. aureus*	[16a]
Ti	Ti-based nanospikes	HT etching	MRSA	[24]
Ti	Nanopillars and nanosheets	Plasma etching and HT etching	*S. aureus* and *P. aeruginosa*	[25]
Ti	TiO_2 nanospikes	Low-temperature HT etching	*E. coli*	[26]
Ti	TiO_2 nanowires and nanosheets	HT etching	*E. coli* and *S. aureus*	[27]
Ti	TiO_2 nanoedges	HT etching and thermal annealing	*S. aureus* and *P. aeruginosa*	[28]
Ti	TiO_2 nanorods	HT reaction	*E. coli* and *S. aureus*	[29]
Ti	ZnO/TiO_2 nanoarray	HT synthesis and low temperature liquid phase method	*E. coli* and *S. aureus*	[30]
Ti6Al4V alloy	TiO_2 nanospikes	Cyclic heat treatment and HT etching	*P. aeruginosa*	[31]
Ti6Al4V alloy	Ti-based nanospikes	HT etching	*S. aureus* and *P. aeruginosa*	[32]
Ti6Al4V alloy	TiO_2 nanopillars	Thermal oxidation	*E. coli*, *S. aureus* and *K. pneumoniae*	[33]
Ti6Al4V alloy	Titanium oxide nanoprotrusions	HT etching	*E. coli*, *S. aureus*, *S. epidermidis*, and *P. aeruginosa*	[34]
Ti6Al4V alloy	Titanium oxide nanospikes	HT etching	*S. aureus* and *P. aeruginosa*	[35]
Ti	TN nanowires	Chemical dissolution nucleation technique	*E. coli* and *S. aureus*	[13]
Ti	ZnO nanorods	Micro-arc oxidation (MAO) and HT treatment	*S. aureus*	[36]
Ti	ZnO@CaP nanorods	HT growth and sol-gel method	*E. coli* and *S. aureus*	[37]
Ti	Al_2O_3@ZnO nanorods	MAO, HT growth and atomic layer deposition (ALD)	*S. aureus*	[38]
Ti	Hybrid ZnO/ PDA/RGDC nanorods	ALD and HT growth	*E. coli* and *S. aureus*	[11b]
Ti	$NaCa_2HSi_3O_9$ nanorods	MAO and HT treatment	*E. coli* and *S. aureus*	[39]
Ti	Hydroxyapatite nanorods	MAO and HT treatment	*S. aureus*	[40]

tomography to observe the morphology of bacteria cultured on TiO_2 nanopillars.[33] Although deformation and penetration are detected from the bacterial envelope, no mechanical disruption or cell lysis is observed (**Figure 2a**) and hence, the results cannot explain the reduced bacterial viability detected on the nanopillar arrays. However, proteomic analyses indicate that the nanopillars can upregulate protein expressions due to oxidative stress and elevate the intracellular H_2O_2 levels in the bacterial cells upon contact (Figure 2b). In fact, oxidation stress in different bacteria with different envelope thicknesses and rigidity contributes to bacterial inactivation, while at the same time, cell lysis becomes less necessary in the antibacterial performance.

2.2. Nanostructures Composed of Other Elements

Besides Ti-based compounds, nanostructured surfaces can be fabricated by crystallizing or depositing with other elements. Nanostructured ZnO, Al_2O_3, $NaCa_2HSi_3O_9$, and hydroxyapatite have been deposited on Ti for antibacterial purposes. For instance, Ye et al. have explored the bactericidal effects of nanorods with different heights and sharpness.[38] Three kinds of nanorods are prepared on the Ti substrate by micro-arc oxidation. The sharp ZnO nanorods have lengths of 469 and 884 nm, and the top-flat hydroxyapatite (HA) nanorods have a length the same as the shorter ZnO sample. To minimize the effects of leaching of Zn^{2+}, roughness, wettability, and zeta potentials, the Al_2O_3 coating on these nanorods is modified by atomic layer deposition (**Figure 3a**). As shown in Figure 3b, the top-flat HA nanorods only eliminate less than 30% *S. aureus* after 24 h incubation but in contrast, both the short and high ZnO nanorods with sharp tops exhibit antibacterial rates of more than 95%, indicating that the top sharpness contributes mostly to the bactericidal effects on closely packed nanoarrays while the effects of heights is negligible. The difference in the antibacterial effect stems from the maximum stress (S_{max}) the nanorods impose on the cell wall of *Staphylococcus aureus (S. aureus)*. As for the sharp nanorod (θ_{top} = 50°), the calculated S_{max} by finite element (FE) simulation is 20.15 MPa (Figure 3d), which is larger than the ultimate-tensile-strength (UTS) of the cell wall (13 MPa). Hence, the top-sharp samples are able to penetrate the cell wall and kill bacteria. In comparison, the top-flat nanorods can only deform the cell wall because S_{max} (5.56 MPa) is less than the UTS (Figure 3c). The relationship between the top angle and S_{max} on the cell wall is studied, and the critical top angle needed by the nanorods to penetrate *S. aureus* is calculated to be 138° (Figure 3e,f). In the in vivo assessment, Ti implants with top-sharp nanorods have excellent mechano-bactericidal properties and osseointegration.

In addition to the bactericidal activity, nanostructures comprising other elements can accentuate the effects with the proper design. For example, nanostructured ZnO surfaces possess both mechano-bactericidal ability and semiconducting characteristics. For example, Wang et al. have fabricated Au-coated ZnO nanorods on Ti to enhance the electron transfer between bacteria

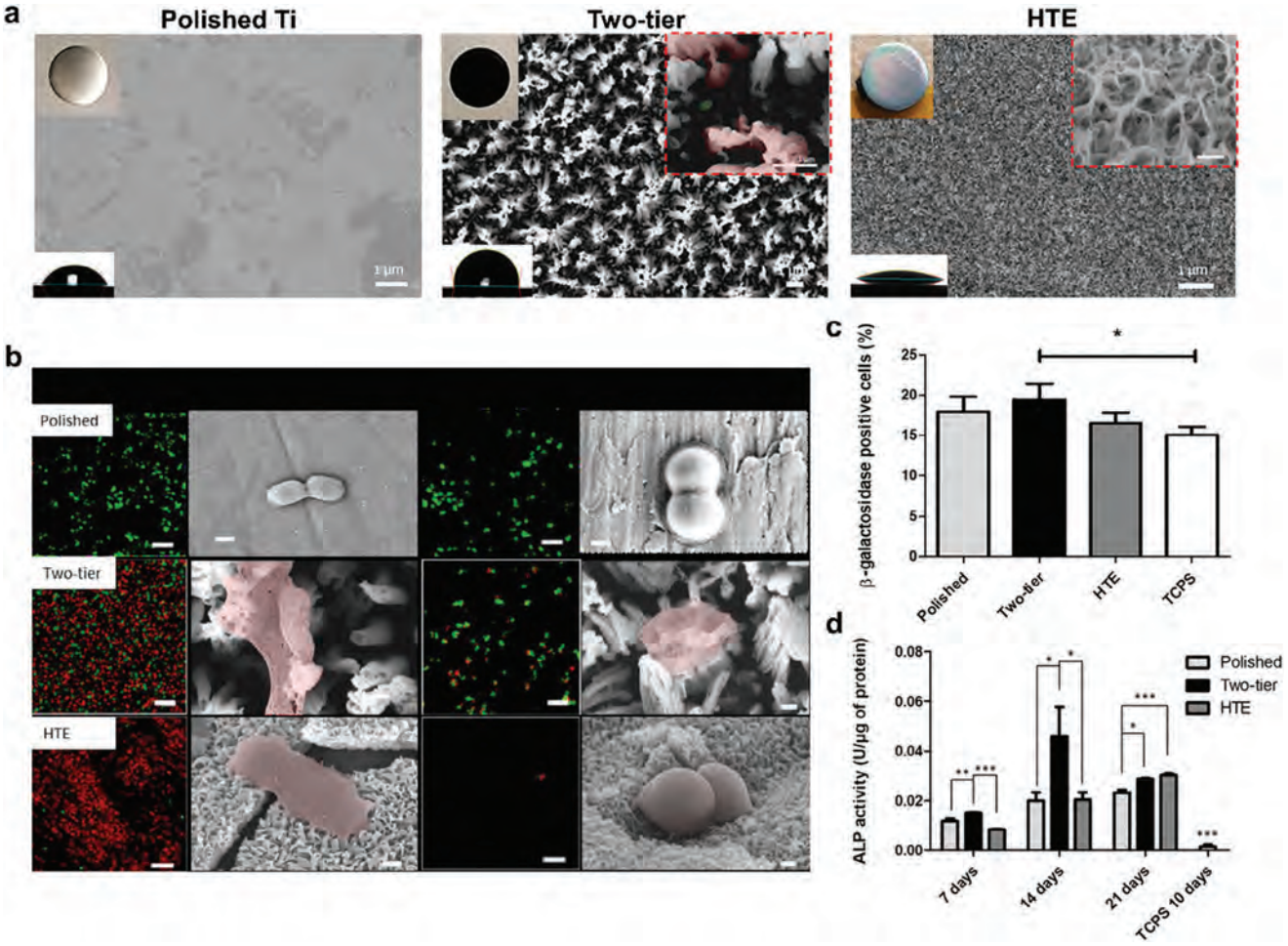

Figure 1. a) Optical images, SEM images, and water contact angle results of Ti after polishing, plasma etching, and HT etching; b) Live/dead staining (scale bar = 10 μm) and SEM images (scale bar = 200 nm) of *P. aeruginosa* and *S. aureus* on the different samples; c) *β*-galactosidase levels of hASCs after culturing for 3 days; d) ALP activity of hASCs after seeding. Reproduced with permission.[25] Copyright 2020, American Chemical Society.

and implant surface, resulting in severe oxidation stress in bacteria and efficient sterilization.[42] In addition, the relationship between the saturation current and bacteria number on the semi-log scale is confirmed using the Au-loaded semiconductor, which also can be used for bacteria sensing.

2.3. Synergistic Strategies

Although mechanical methods can potentially eliminate bacteria without antibiotics, a single nanostructure may not be able to sterilize all pathogens, especially Gram-positive bacteria with rigid cell walls.[43] As mentioned in the previous section, the cell wall of *S. aureus* cannot be penetrated by Al_2O_3@ZnO nanorods unless the top angle of the nanorods is less than 138°,[38] consequently increasing the difficulties in sample preparation. To maximize the bactericidal ability of nanostructured surfaces, synergistic strategies have been developed in conjunction with antibiotics,[34] antimicrobial peptides,[40,44] lysozyme,[39] photothermal therapy (PTT),[29] as well as photodynamic treatment (PDT).[29,45] In fact, nanostructured surfaces can be complementary to other antibacterial treatments to enhance their efficacy. Although the cell wall of Gram-positive bacteria cannot be easily penetrated by nanoprotrusions, the inner layers of peptidoglycan are exposed as a result of membrane deformation to increase the binding probability of specific drugs. Furthermore, nanostructures can be penetrated more effectively by increasing the membrane permeability through hyperthermia or Zn treatment,[11b,29] thereby improving the efficiency of eliminating Gram-positive bacteria.

Bright et al. have investigated the synergistic effects between the sharp nanostructured Ti surface and clinically used antibiotics.[34] In the presence of a hydrothermally etched Ti (HTE-Ti) surface, vancomycin is capable of eradicating the *S. aureus* biofilm with a dosage lower than that used clinically, whereas limited anti-biofilm activity is observed after a single HTE-Ti or antibiotic treatment (**Figure 4a**). The synergistic effects between vancomycin and nanostructured HTE-Ti are ascribed to two reasons. First, compared to the orderly *S. aureus* on titanium (AR-Ti), bacteria cultured on the HTE-Ti surface show a distorted shape due to the mechanical interactions between the cell walls and sharp nanoprotrusions (Figure 4b). Owing to the deformation of *S. aureus*, the peptidoglycan layer can be better exposed to

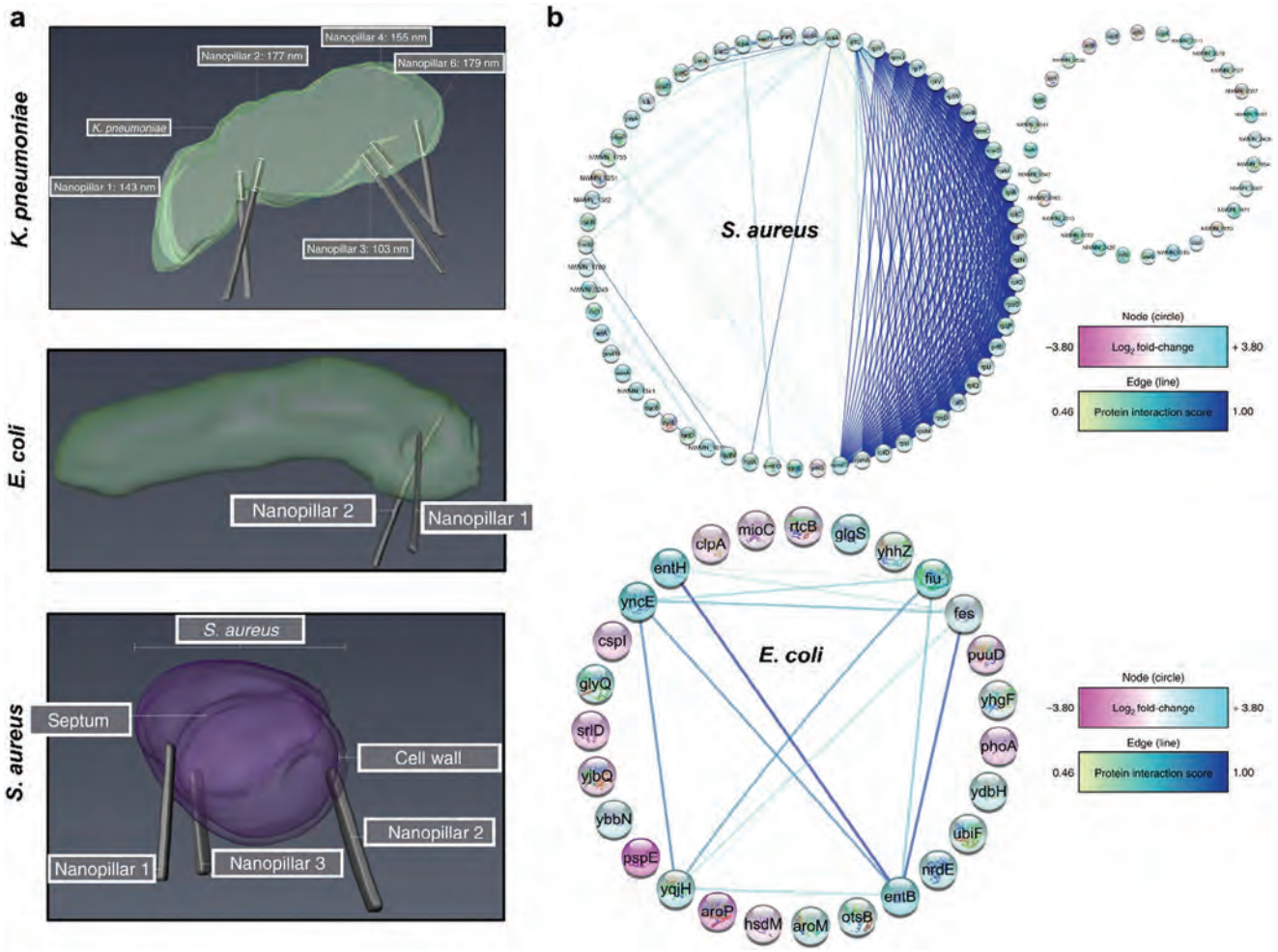

Figure 2. a) Electron tomography analysis of *K. pneumoniae* and automated FIB-SEM cross-sectional analysis of *E. coli* and *S. aureus* after contacting the TiO_2 nanopillars; b) Proteomic analyses indicating that the protein expressions related to oxidation stress of *S. aureus* and *E. coli* are altered in the presence of TiO_2 nanopillars. Reproduced with permission.[33] Copyright 2020, Springer Nature.

promote the binding between vancomycin and the d-Ala-d-Ala component of peptidoglycan.[46] Meanwhile, since the damaged cell wall needs to be repaired, vancomycin may bind with peptidoglycan more effectively during biosynthesis and also impede cross-linkage of new peptidoglycan,[46a,47] consequently improving the utilization of antibiotics and inhibiting cell wall reinforcement. Second, the oxidative stress triggered by mechanical deformation is amplified by vancomycin that suppresses catalase production. As shown in Figure 4c,d, the intracellular H_2O_2 concentration and catalase-related gene (*katA*) are upregulated after treating *S. aureus* with HTE-Ti for 7 days, furnishing evidence that the oxidative stress produced by the nanostructured surface and gene expression mitigates the physiological disorder. In the presence of vancomycin, *katA* expression is inhibited, and the intracellular H_2O_2 starts to accumulate (Figure 4c,e), leading to amplified oxidation stress and bacterial inactivation thereafter. Therefore, the mechano-bactericidal effects of nanostructured surfaces can be exploited in combination with other treatments to improve the antibacterial efficacy.

3. Mg-Based Biomaterials and Implants

Mg is another popular metal in orthopedics research because of its biodegradable behavior,[48] density similar to that of human calvarium bone,[49] and lower elastic modulus for mitigation of stress shielding.[50] During degradation, Mg ions released from Mg-based implants participate in hydroxyapatite deposition and accelerate new bone formation.[51] Recently, Bioretec Ltd. announced that their Mg-based trauma screw (RemeOs series) was approved by US FDA as the first bioresorbable metal implant for ankle fracture repair, which increases the application prospects of Mg-based metals to orthopedic implants. Nevertheless, studies on mechano-bactericidal surfaces on Mg-based metals have been scarce compared to Ti-based metals. This is because the degradation products of Mg are inherent antimicrobials,[52] which decreases the demand for designing antibacterial Mg-based implants. Although some nano-topographies like vertical nanosheets and nanospikes have been fabricated on Mg-based metals, less attention has been paid to their mechano-bactericidal ability.[53] Instead, there has been more focus on how to improve

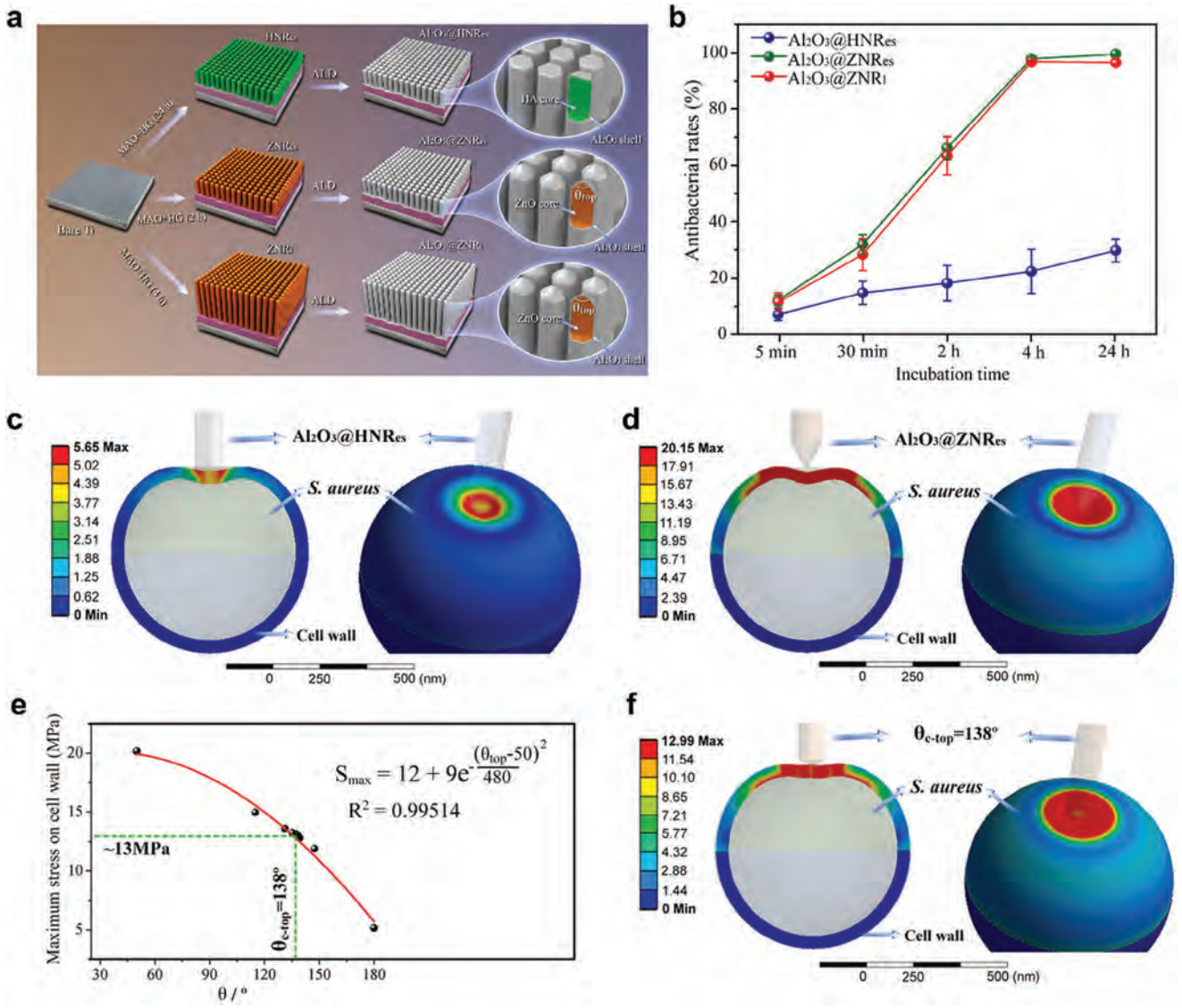

Figure 3. a) Schematic diagram showing the fabrication of nanorods arrays with different heights and top sharpness; b) Antibacterial rates showing the significant bactericidal actions on the top-sharp nanorods; Different cell wall stress imposed by c) Top-flat and d) Top-sharp nanorods; e) Curve and formula showing the relationship between top angle and S_{max} imposed to cell wall; f) FE simulation showing that the critical top angle of nanorods needed to penetrate the cell wall is 138°. Reproduced with permission.[38] Copyright 2022, Elsevier.

the corrosion resistance of Mg as rapid degradation degrades the mechanical properties and can create a toxic biological environment due to the accumulation of corrosion by-products.[54]

Wang et al. have designed a nanostructured surface on Mg by in situ construction of 2D $Mg(OH)_2$ nanoflakes (designated as HT12),[55] which can inactivate the bacteria due to the mechano-disrupting action that is different from the antibacterial mechanism of pure Mg by generating environmental stress. As shown in **Figure** 5a, the bacteria on the Mg surface are shriveled (white arrows) due to the large Mg^{2+} concentration and alkaline environment produced by Mg degradation. Owing to the protection of low-soluble $Mg(OH)_2$, Mg^{2+} release and alkaline conditions are relieved on HT12 (Figure 5b,c) to decrease the environmental stress on the bacteria. Nevertheless, the viability of bacteria is damaged after culturing on HT12, and the bacterial membranes are invaginated and stretched, which is indicative of the fatal mechanical interactions between the nanoflakes and membranes. Theoretical simulation reveals that the membrane area increases when the surface tension exerted on the membrane exceeds 30 dyne cm^{-1} (Figure 5e). Hence, HT12 exerting 40.5 dyne cm^{-1} shows a broadened bilayer and a 30% increase in the area per lipid after interacting with the lipid bilayer for 200 ns (Figure 5f), consequently destroying the membrane structure and inactivating the bacteria. Furthermore, the all-atom model simulation shows no significant change in the lipid bilayer in the presence of $Mg(OH)_2$ and H_2O, demonstrating that antibacterial actions are realized by physical force instead of a hypertonic environment. Owing to the mechano-bactericidal ability and improved corrosion resistance, HT12 can eliminate bacteria in vivo without causing an inflammatory response.

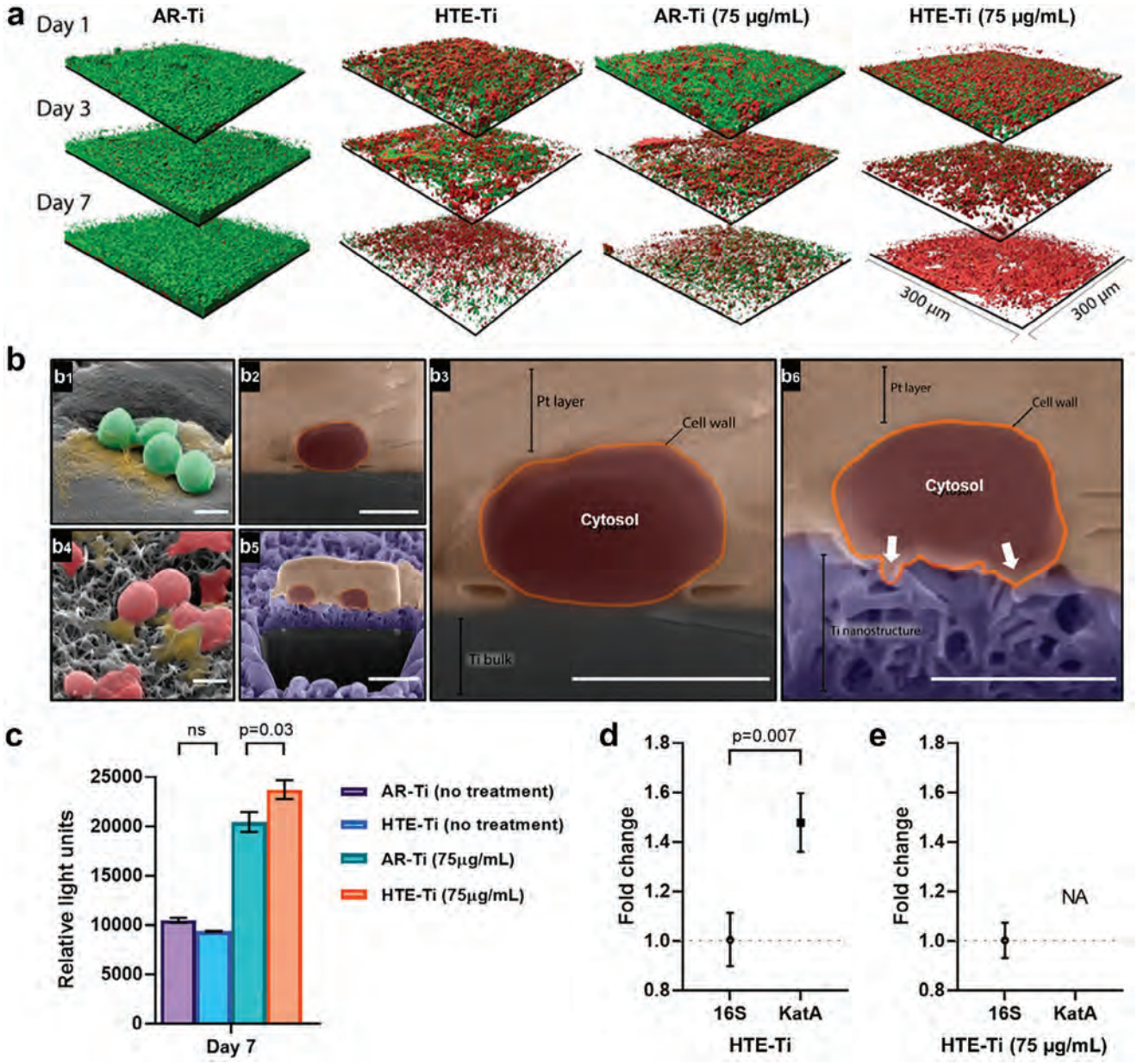

Figure 4. a) Enhanced anti-biofilm effects detected from the combination of nanostructured HTE-Ti and vancomycin; b1–b3) 52° tilted and cross-sectional SEM images of the well-shape *S. aureus* on AR-Ti; b4–b6) 52° tilted and cross-sectional SEM images of the distorted *S. aureus* on HTE-Ti; c) Upregulated H_2O_2 level detected from *S. aureus* treated with HTE-Ti and vancomycin for 7 days; KatA expressions in *S. aureus* cultured on HTE-Ti d) With and e) Without adding vancomycin. Reproduced with permission.[34] Copyright 2022, American Chemical Society.

4. Polyether-Ether-Ketone

PEEK, a member of the polyaryletherketone family, is a popular polymer for orthopedic implants on account of its unique mechanical and stable properties.[56] PEEK contains connected ketone and ether functional groups between aromatic rings.[57] Compared to metals, the mechanical properties of PEEK, such as the tensile modulus, flexural modulus, and compressive modulus, are closer to those of the natural cortical bone.[58] Owing to the long-term stability, no ions are released from PEEK and there are fewer inflammatory responses.[59] PEEK has been approved by the US FDA as a medical implant since the end of the 20th century,[60] and various commercial products have been developed for interspinous process decompression,[61] spinal fusion,[62] and cranial/craniofacial reconstruction. However, PEEK is biologically inert and chemically stable, implying a lack of antibacterial properties and difficulties in fabricating mechano-bactericidal surfaces.[63] Concentrated sulfuric acid can be used to fabricate an antibacterial 3D nanonetwork on the surface of PEEK, but the bactericidal actions are attributed to sulfur

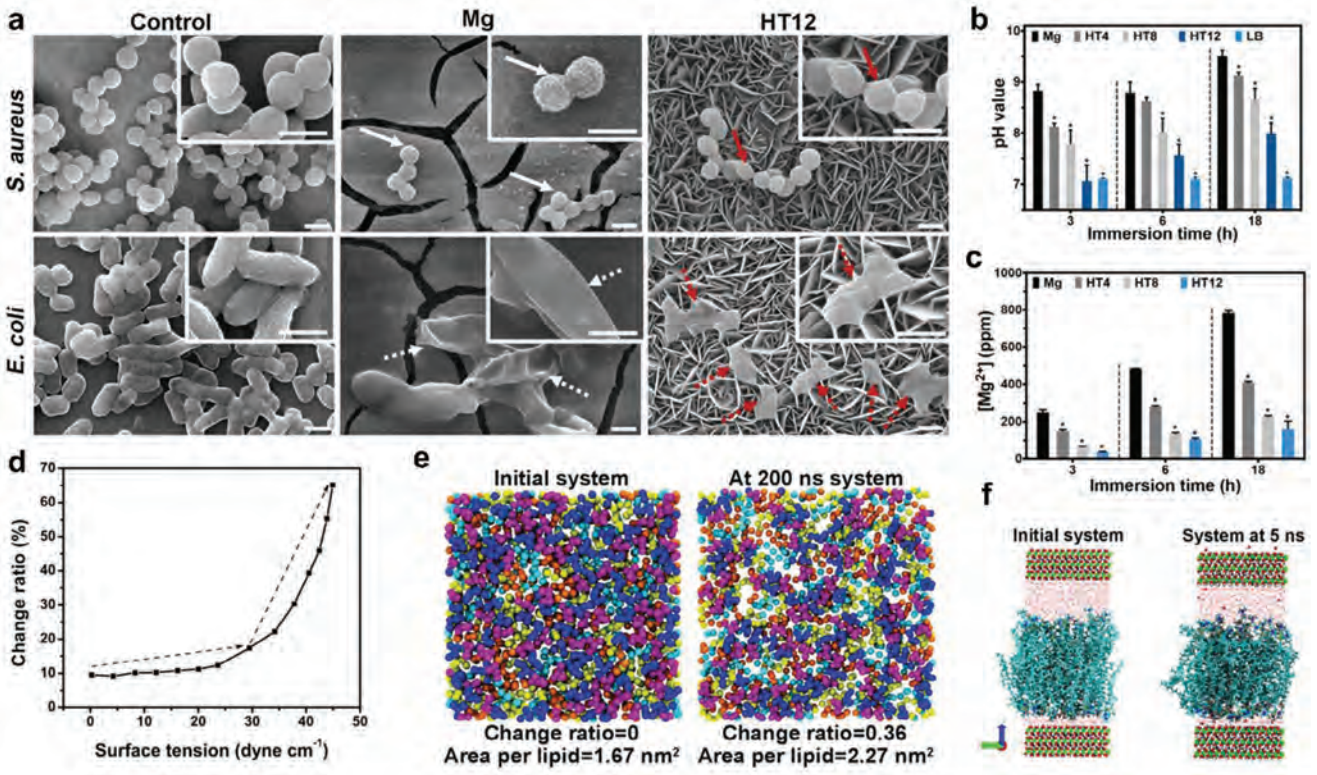

Figure 5. a) Bacterial morphology of *S. aureus* and *E. coli* cultured on different sample surfaces; Changes in b) pH value and c) Mg^{2+} concentrations after immersing the samples in the LB medium for 3, 6, and 18 h; d) Changes of the ratios of the bilayer area with surface tension; e) Theoretical simulation showing that HT12 exerting 40.5 dyne cm^{-1} surface tension increases 30% of the area per lipid in the bilayer after in contact for 200 ns; f) All-atom simulation showing that the lipid bilayer is not damaged in presence of $Mg(OH)_2$ and H_2O. Reproduced with permission.[55] Copyright 2020, Wiley.

diffusion instead of physical forces.[64] To endow PEEK with antibacterial properties, Chen et al. have prepared ZnO nanorods on PEEK to monitor the loading and releasing behavior of antibiotics without mentioning the antibacterial effects of nanostructured surfaces.[65]

Template printing can be utilized to prepare ordered nanopillar arrays on PEEK. Ye et al. have filled anodic aluminum oxide (AAO) nanotubes with melted PEEK and removed the AAO template after PEEK cures to obtain a nanostructured PEEK surface with long-term bactericidal effects.[66] The plasma technique is also favorable to fabricating nanostructured surfaces on PEEK because the conditions can be adapted to the physical properties of polymer materials, thus causing less damage.[67] After Ti plasma ion implantation, TiO_2 nanopores formed on the carbon-fiber-reinforced PEEK inhibit bacteria adhesion by reducing the available substrata-bacteria contact area.[68] As for the bacteria-killing effects, Mo et al. have combined plasma etching with the template method to construct micro and nanopatterns on PEEK with different antibacterial mechanisms.[69] Under a polystyrene (PS) monolayered mask, a cone-like structure is formed on the surface after O_2 plasma etching, while a pillar-like morphology emerges after Ar and O_2 plasma etching. The differences in the morphology stem from the different etching rates between PEEK and PS, as PEEK can be etched by Ar and O_2 plasmas but PS can only be etched by the O_2 plasma. Accordingly, the antibacterial effects of microcones and micropillars are attributed to physical stretching and dimensional effect, while cone-like and pillar-like nanopatterns can penetrate the membrane to inactivate bacteria.

PEEK with nanostructured surfaces can also be fabricated by plasma etching due to the semicrystalline characteristics. Mo et al. have found that the amorphous phase in PEEK can be preferentially removed by the Ar plasma to form a vertical nanolamella surface (denoted as P-VL).[70] In addition, the nanolamella structure is tilted (denoted as P-TL) if the pre-annealing is conducted before Ar plasma etching (**Figure 6**a). The changes in the angle of the nanolamellae arise from chain relaxation/movement and rearrangement/crystallization of PEEK after annealing. Interestingly, P-VL and P-TL exhibit different antibacterial behavior and osteogenic ability. As for the P-VL, the sharp and vertical nanolamellae pierce the bacterial membrane to sterilize the bacteria (Figure 6b), but in contrast, P-TL shows enhanced affinity to bacteria and disrupts the membrane by stretching as the bacteria move (Figure 6b,c). In the P-TL group, better osteoblast attachment and proliferation are detected due to the improved hydrophilicity and surface roughness, and the side effects of the nanolamella structure are also mitigated compared to the vertical nanolamellae (Figure 6d). Therefore, the P-TL with the optimal nanostructure not only eliminates bacterial infection, but also promotes new bone formation as confirmed by defects in rat tibia (Figure 6e).

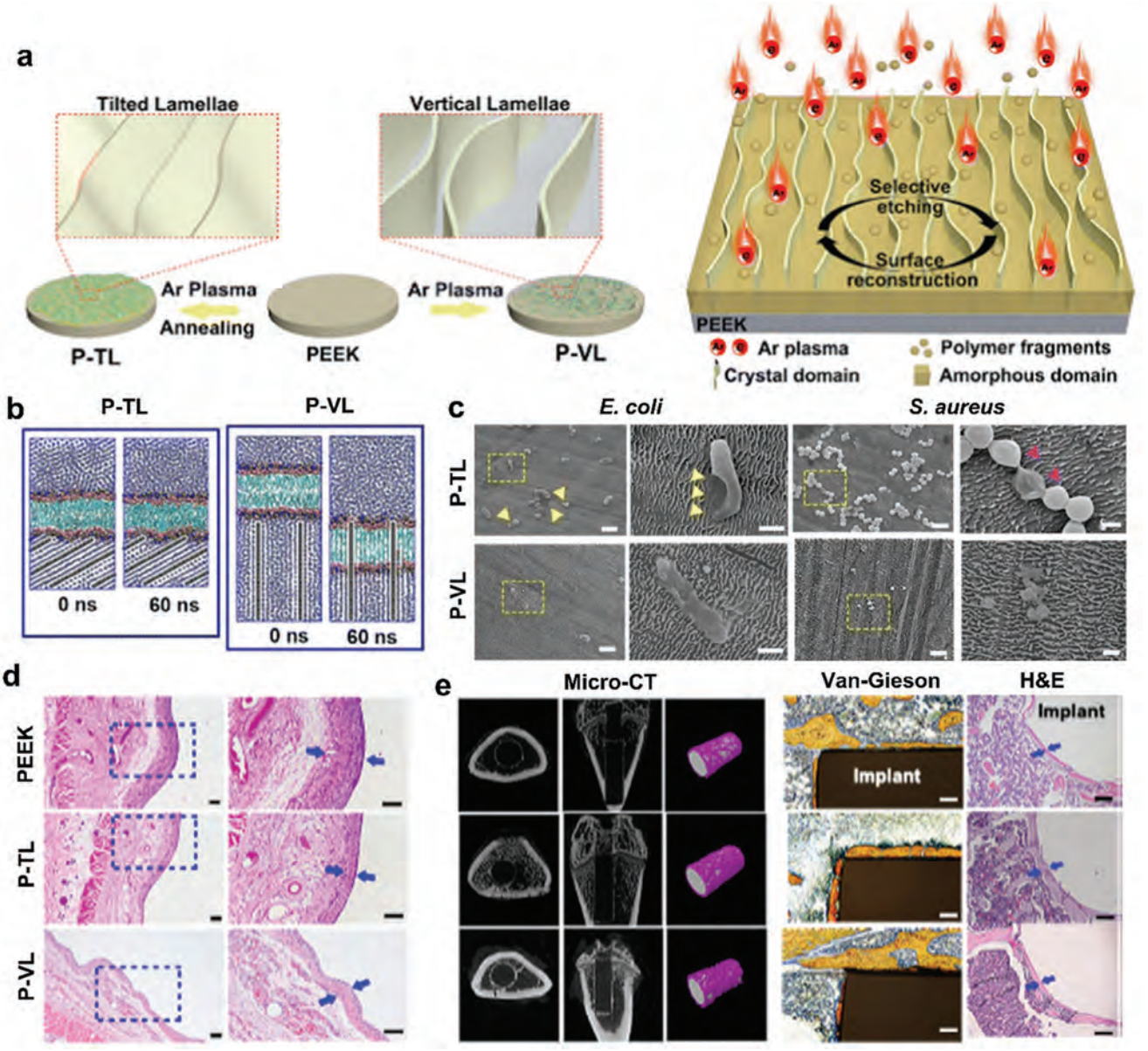

Figure 6. a) Schematic diagram showing the preparation of vertical and tilted nanolamellae on PEEK; b) Molecular dynamics simulation showing different mechanical stresses exerted by P-TL and P-VL on the bacterial membrane; c) SEM images showing different membrane disruption caused by P-TL and P-VL (Scale bars = 2 μm and 500 nm); d) H&E staining images of the peri-implant tissues indicating the in vivo bactericidal ability of P-TL and P-VL (Scale bar = 200 μm); e) Micro-CT, Van–Gieson and H&E staining images showing that osteointegration of P-TL is better than that of P-VL (Scale bar = 200 μm). Reproduced from Ref.[70] with permission from the Royal Society of Chemistry. Copyright 2023.

5. Outlook

Due to the high occurrence of SSIs and AMR, alternative antibacterial strategies need to be developed to reduce the overuse of antibiotics while considering biosafety.[71] Surface modification based on chemical methods is also a common strategy to endow biomaterials with antibacterial activity in which antimicrobials are covalently grafted onto the substrate surface.[72] However, common orthopedic materials usually lack sufficient surface reactivity to allow direct linkage with biomacromolecules, consequently increasing the difficulties in product preparation and commercialization. On the contrary, mechano-bactericidal strategies show less dependence on the chemical reactivity of materials because the nanostructures can be formed by various techniques including crystal growth, physical etching, and so on. Meanwhile, nanostructured surfaces on biomedical materials not only mechanically inactivate bacteria, but also modulate the differentiation of stem cells to facilitate the treatment of peri-implant bacterial infections.[73] As aforementioned, the development of mechano-bactericidal surfaces varies with different

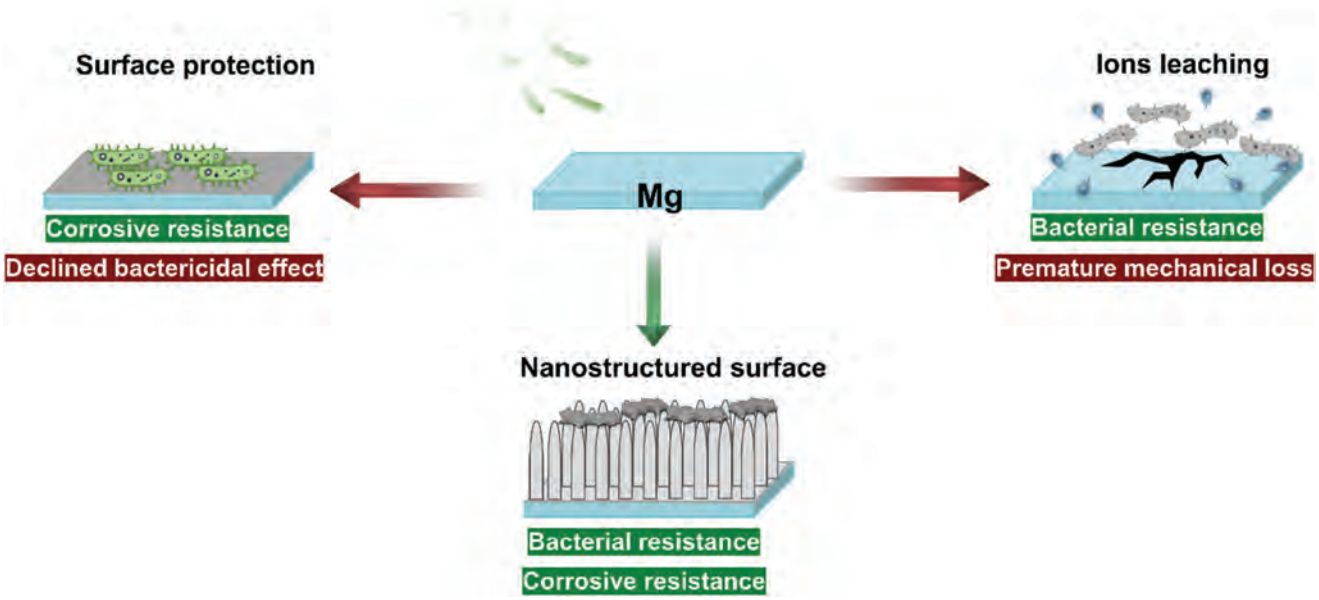

Figure 7. Schematic diagram indicating the potential of nanostructured surfaces to reduce corrosion and retain the bacterial resistance of Mg-based metals.

substrates and among the three materials described here, Ti-based implants are more popular than Mg-based metals and PEEK. The relative lack of research on mechano-bactericidal surfaces on Mg-based materials may, in part, be due to the intrinsic antibacterial properties of Mg because the degradation products can inactivate bacteria. Hence, there has been more attention on the corrosion resistance of Mg in order to prevent premature loss of mechanical strength before tissue recovery and inflammatory response. However, slower corrosion produces less Mg^{2+} and OH^-, and the antibacterial effects can be compromised.[74] Establishing a dual corrosion-resistant and mechano-bactericidal surface is a promising solution (**Figure 7**). The nanostructured surface not only protects the substrate, but also inactivates pathogens via the mechanism of contact-killing for Mg-based implants. Moreover, unlike other commercial clinical biomaterials, Mg-based orthopedic products were approved by the US FDA only in 2023. It is believed that this dual strategy will receive more research interest in the future.

The difficulties in preparing nanopatterns on PEEK are related to the strong solvent stability, as only concentrated acids can attack PEEK at room temperature.[75] Besides, PEEK is soluble only in high-boiling-point organic solvents at a temperature close to its melting point.[75b,76] Therefore, common surface etching methods for metals are not suitable for PEEK. Moreover, the inorganic nanostructures produced chemically may not adhere well to the polymer substrate, giving rise to the collapse of the nanotopography. Plasma etching is a proper technique to modify PEEK, but the demands for the apparatus and conditions are more stringent than those in chemical methods. Since PEEK has a melting point much lower than that of other medical metals, molds can be designed for plastic injection to produce nanostructures on PEEK during manufacturing. Furthermore, substrate-independent methods can be utilized to produce nanostructured surfaces. For instance, Zhang et al. have prepared a smart polyimide coating with integrated mechanical and antimicrobial characteristics that can bond well with commercial implants with the aid of thermally curable polyurethane and medical adhesive tape.[77] In this case, the importance of the material composition and reactivity of substrates decreases and as a result, universal bactericidal nanopatterns can be prepared on different implants.

In addition to the preparation methods, there are two potential constraints of the mechano-bactericidal strategies for orthopedic SSIs. First of all, surface nanopatterns may be destroyed by peri-implant mechanical attack because orthopedic implants usually need to bear weight or are subjected to friction from adjacent tissues and joints.[78] Therefore, these nanostructures can collapse if they do not adhere well to the substrate. In some cases, the detached debris may induce local inflammatory responses[79] and hinder osteogenesis.[80] Therefore, how to preserve the structural stability of the nanomorphology in a complex mechanical environment in vivo must be addressed. Second, direct contact and enhanced binding between bacteria and nanostructured surfaces are the primary mechanisms in mechano-mediated sterilization. However, dead bacteria can stick to the implant surface to shield the nanopatterns. Although the debris is released gradually after inactivation for ≈20 min,[81] bacteria still have the chance to attach and colonize on the shielded surface[35] to cause infection (**Figure 8**). In this respect, Liu et al. have grafted salt-responsive polyzwitterionic (polyDVBAPS) brushes on the nanostructured surfaces to release the inactivated bacteria.[82] The bacteria are killed mechanically by the nanopatterns under the condition of low ionic strength. After switching to a high ionic concentration, the grafted polyDVBAPS brushes extend and repel the bacterial debris from the surface. In the future, new stimuli and methods with clinical viability will be researched to trigger bacteria release from mechano-bactericidal surfaces.

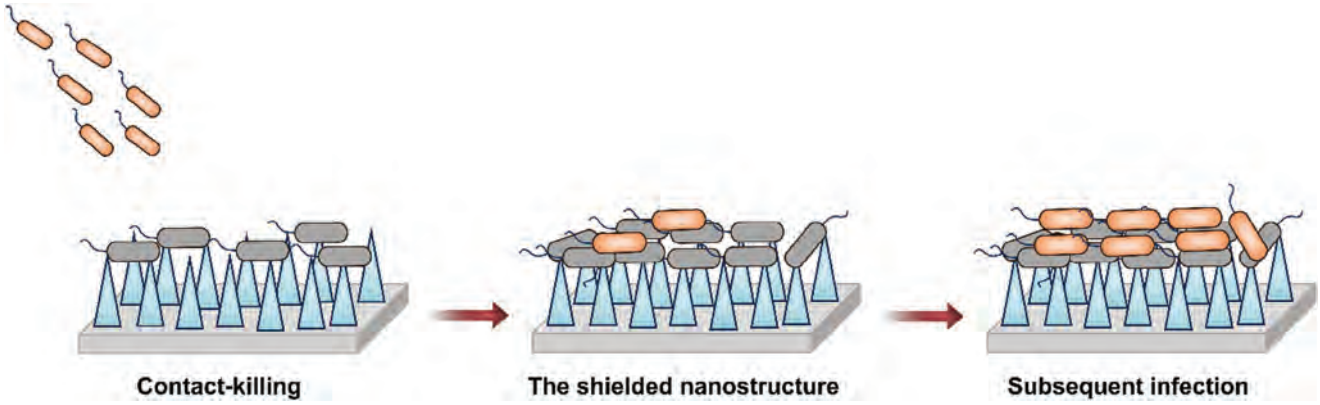

Figure 8. Schematic diagram showing the topography-shielding effect due to bacterial debris on the nanostructured surfaces.

6. Conclusion

This review summarizes the latest advances pertaining to mechano-bactericidal surfaces on orthopedic implants by focusing on three FDA-approved materials (Ti, Mg, and PEEK). The different developments and requirements for the three materials are described and the potential methods and techniques to improve the various characteristics are discussed. Nanostructured surfaces can modulate cell behavior and mechanically sterilize bacteria without administering antibiotics, thus avoiding the emergence of superbugs and other medical complications. However, current mechano-bactericidal strategies are not perfect for orthopedic implants as the morphological stability in complex mechanical environments and nanopattern shielding caused by bacteria debris must be addressed in-depth. It is expected that mechano-bactericidal strategies will attract much research interest in the future to bring them to clinical fruition.

Acknowledgements

This work was supported by City University of Hong Kong Donation Research Grants (DON-RMG 9229021 and 9220061), Hong Kong PDFS–RGC Postdoctoral Fellowship Scheme (PDFS2122-1S08 and CityU 9061014), as well as Hong Kong HMRF (Health and Medical Research Fund) (2120972 and CityU 9211320).

Conflict of Interest

The authors declare no conflict of interest.

Keywords

magnesium, mechano-bactericidal surfaces, nanostructured surfaces, orthopedic implants, polyether-ether-ketone, titanium

Received: January 2, 2024
Revised: January 24, 2024
Published online: February 9, 2024

[1] R. McEntee, S. Rengifo, D. Pedowitz, A. M. Ilyas, *SurgiColl* **2023**, *1*, 00008.
[2] a) Q. Liu, W. Li, Y. Qian, C. Wang, P. Xia, *The Innovation Life* **2023**, *1*, 100012; b) D. Boraschi, A. Tagliabue, *The Innovation Life* **2023**, *1*, 100025; c) Y. Du, L. Liu, W. Ma, W. Yan, W. Mao, Y. Du, K. Cui, P. Yu, Z. Li, P. J. Sansonetti, *The Innovation Life* **2023**, *1*, 100016.
[3] G. K. Upadhyyaya, S. Tewari, G. K. Upadhyaya, *Cureus* **2023**, *15*, e47828.
[4] T. Cieplak, N. Soffer, A. Sulakvelidze, D. S. Nielsen, *Gut Microbes* **2018**, *9*, 391.
[5] a) Y. Wu, H. Wang, P. Chu, *The Innovation Life* **2023**, *1*, 100027; b) L. Wang, Y. Zhang, J. Xu, Q. Shi, Y. Peng, C. Long, L. Li, Y. Yin, *The Innovation Life* **2023**, *1*, 100022.
[6] Y. Xu, Y. Li, A. Gao, P. K. Chu, H. Wang, *The Innovation Life* **2023**, *1*, 100015.
[7] a) Y. Z. Wu, P. Liu, B. Mehrjou, P. K. Chu, *Adv. Mater.* **2023**, 2305940; b) Y. Z. Wu, Q. Liao, L. Wu, Y. X. Luo, W. Zhang, M. Guan, H. B. Pan, L. P. Tong, P. K. Chu, H. Y. Wang, *ACS Nano* **2021**, *15*, 17854.
[8] D. P. Linklater, V. A. Baulin, S. Juodkazis, R. J. Crawford, P. Stoodley, E. P. Ivanova, *Nat. Rev. Microbiol.* **2021**, *19*, 8.
[9] E. P. Ivanova, J. Hasan, H. K. Webb, V. K. Truong, G. S. Watson, J. A. Watson, V. A. Baulin, S. Pogodin, J. Y. Wang, M. J. Tobin, C. Löbbe, R. J. Crawford, *Small* **2012**, *8*, 2489.
[10] M. Michalska, F. Gambacorta, R. Divan, I. S. Aranson, A. Sokolov, P. Noirot, P. D. Laible, *Nanoscale* **2018**, *10*, 6639.
[11] a) Y. Z. Wu, D. Z. Xiao, P. Liu, Q. Liao, Q. D. Ruan, C. Huang, L. L. Liu, D. Li, X. L. Zhang, W. Li, K. W. Tang, Z. W. Wu, G. M. Wang, H. Y. Wang, P. K. Chu, *Research* **2023**, *6*, 0074; b) J. Li, L. Tan, X. M. Liu, Z. D. Cui, X. J. Yang, K. W. K. Yeung, P. K. Chu, S. L. Wu, *ACS Nano* **2017**, *11*, 11250; c) F. Zhao, A. Gao, Q. Liao, Y. Li, I. Ullah, Y. Zhao, X. Ren, L. Tong, X. Li, Y. Zheng, *Adv. Funct. Mater.* **2024**, 2311812.
[12] I. Izquierdo-Barba, J. M. García-Martín, R. Alvarez, A. Palmero, J. Esteban, C. Pérez-Jorge, D. Arcos, M. Vallet-Regí, *Acta Biomater.* **2015**, *15*, 20.
[13] G. M. Wang, K. W. Tang, W. J. Jiang, Q. Liao, Y. Li, P. Liu, Y. Z. Wu, M. T. Liu, H. Y. Wang, B. Li, J. Z. Du, P. K. Chu, *Adv. Mater.* **2023**, *35*, 2212315.
[14] V. T. H. Pham, V. K. Truong, M. D. J. Quinn, S. M. Notley, Y. C. Guo, V. A. Baulin, M. Al Kobaisi, R. J. Crawford, E. P. Ivanova, *ACS Nano* **2015**, *9*, 8458.
[15] X. Li, K. H. Tsui, J. K. H. Tsoi, D. W. Green, X. Z. Jin, Y. Q. Deng, Y. M. Zhu, X. G. Li, Z. Y. Fan, G. S. P. Cheung, *Nanoscale* **2020**, *12*, 18864.
[16] a) Q. Gao, T. Feng, D. N. Huang, P. Liu, P. Lin, Y. Wu, Z. M. Ye, J. Ji, P. Li, W. Huang, *Biomater. Sci.* **2020**, *8*, 278; b) B. Mehrjou, S. Mo, D. Dehghan-Baniani, G. M. Wang, A. M. Qasim, P. K. Chu, *ACS Appl. Mater. Interfaces* **2019**, *11*, 31605; c) G. Hazell, L. E. Fisher, W. A. Murray, A. H. Nobbs, B. Su, *J. Colloid Interf. Sci.* **2018**, *528*, 389.

[17] C. R. Arciola, D. Campoccia, L. Montanaro, *Nat. Rev. Microbiol.* **2018**, *16*, 397.
[18] V. T. H. Pham, V. K. Truong, A. Orlowska, S. Ghanaati, M. Barbeck, P. Booms, A. Fulcher, C. M. Bhadra, R. Buividas, V. Baulin, C. J. Kirkpatrick, P. Doran, D. E. Mainwaring, S. Juodkazis, R. J. Crawford, E. P. Ivanova, *ACS Appl. Mater. Inter* **2016**, *8*, 22025.
[19] K. Palka, R. Pokrowiecki, *Adv. Eng. Mater.* **2018**, *20*, 1700648.
[20] C. R. Razavi, P. J. Byrne, *Facial Plast. Surg.* **2023**, *39*, 460.
[21] G. Van Acker, J. Belding, C. H. Kim, *Sacroiliac Joint Pain: A Comprehensive Guide to Interventional and Surgical Procedures*, Oxford Academic, New York, **2021**.
[22] R. Khalaj, A. G. Tabriz, M. I. Okereke, D. Douroumis, *Int. J. Pharmaceut.* **2021**, *609*, 121153.
[23] L. Z. Ping, C. Z. Yuan, Y. M. Yan, Y. W. Song, *Biomed. Environ. Sci.* **2023**, *36*, 983.
[24] J. V. Wandiyanto, S. Cheeseman, V. K. Truong, M. Al Kobaisi, C. Bizet, S. Juodkazis, H. Thissen, R. J. Crawford, E. P. Ivanova, *J. Mater. Chem. B* **2019**, *7*, 4424.
[25] T. Le Clainche, D. Linklater, S. Wong, P. Le, S. Juodkazis, X. L. Guevel, J. L. Coll, E. P. Ivanova, V. Martel-Frachet, *ACS Appl. Mater. Interfaces* **2020**, *12*, 48272.
[26] J. Morel, O. Mcneilly, S. Grundy, T. Brown, C. Gunawan, R. Amal, J. A. Scott, *ACS Appl. Mater. Inter* **2023**, *15*, 46247.
[27] L. D. Zhao, T. Q. Liu, X. Q. Li, Q. Q. Cui, Q. Q. Wu, X. Wang, K. D. Song, D. Ge, *ACS Biomater. Sci. Eng.* **2021**, *7*, 2268.
[28] J. V. Wandiyanto, T. Tamanna, D. P. Linklater, V. K. Truong, M. Al Kobaisi, V. A. Baulin, S. Joudkazis, H. Thissen, R. J. Crawford, E. P. Ivanova, *J. Colloid Interf. Sci.* **2020**, *560*, 572.
[29] X. Y. Zhang, G. N. Zhang, M. Z. Chai, X. H. Yao, W. Y. Chen, P. K. Chu, *Bioact Mater* **2021**, *6*, 12.
[30] S. M. Pang, Y. He, R. Zhong, Z. Z. Guo, P. He, C. R. Zhou, B. Xue, X. J. Wen, H. Li, *Ceram. Int.* **2019**, *45*, 12663.
[31] A. Mathew, J. Hasan, S. Singamneni, P. K. D. V. Yarlagadda, *Adv. Eng. Mater.* **2023**, *25*, 2201306.
[32] R. Bright, A. Hayles, D. Fernandes, R. M. Visalakshan, N. Ninan, D. Palms, A. Burzava, D. Barker, T. Brown, K. Vasilev, *ACS Appl. Mater. Inter* **2021**, *13*, 38007.
[33] J. Jenkins, J. Mantell, C. Neal, A. Gholinia, P. Verkade, A. H. Nobbs, B. Su, *Nat. Commun.* **2020**, *11*, 1626.
[34] R. Bright, A. Hayles, J. Wood, D. Palms, T. Brown, D. Barker, K. Vasilev, *Nano Lett.* **2022**, *22*, 6724.
[35] R. Bright, D. Fernandes, J. Wood, D. Palms, A. Burzava, N. Ninan, T. Brown, D. Barker, K. Vasilev, *Mater Today Bio* **2022**, *13*, 100176.
[36] J. Ye, B. Li, M. Li, Y. F. Zheng, S. L. Wu, Y. Han, *Bioact Mater* **2022**, *11*, 181.
[37] I. Ullah, P. Ou, L. Xie, Q. Liao, F. Zhao, A. Gao, X. Ren, Y. Li, G. Wang, Z. Wu, *Acta Biomater.* **2024**, *175*, 382.
[38] J. Ye, B. Li, Y. F. Zheng, S. L. Wu, D. F. Chen, Y. Han, *Bioact Mater* **2022**, *15*, 173.
[39] Y. Xue, J. Chen, L. Zhang, Y. Han, *J. Mater. Sci. Technol.* **2021**, *88*, 240.
[40] K. Li, J. Chen, Y. Xue, T. X. Ding, S. B. Zhu, M. T. Mao, L. Zhang, Y. Han, *Chem. Eng. J.* **2021**, *423*, 130133.
[41] V. C. Anitha, A. N. Banerjee, S. W. Joo, B. K. Min, *Nanotechnology* **2015**, *26*, 355705.
[42] G. M. Wang, K. W. Tang, Z. Y. Meng, P. Liu, S. Mo, B. Mehrjou, H. Y. Wang, X. Y. Liu, Z. W. Wu, P. K. Chu, *Adv. Mater.* **2020**, *32*, 202003616.
[43] N. Lin, P. Berton, C. Moraes, R. D. Rogers, N. Tufenkji, *Adv. Colloid Interface Sci.* **2018**, *252*, 55.
[44] a) J. Huo, Q. Jia, K. Wang, J. Chen, J. Zhang, P. Li, W. Huang, *Langmuir* **2023**, *39*, 1238; b) L. Zhang, Y. Xue, S. Gopalakrishnan, K. Li, Y. Han, V. M. Rotello, *ACS Appl. Mater. Interfaces* **2021**, *13*, 28764.
[45] M. G. Yang, S. Qiu, E. Coy, S. J. Li, Y. Zhang, H. B. Pan, G. C. Wang, *Adv. Mater.* **2022**, *34*, 202106314.
[46] a) F. Wang, H. Y. Zhou, O. P. Olademehin, S. J. Kim, P. Tao, *ACS Omega* **2018**, *3*, 37; b) V. Dengler, P. S. Meier, R. Heusser, B. Berger-Bächi, N. McCallum, *BMC Microbiol.* **2011**, *11*, 16.
[47] H.-K. Kang, Y. Park, *Journal of Bacteriology and Virology* **2015**, *45*, 67.
[48] J. L. Wang, J. K. Xu, C. Hopkins, D. H. K. Chow, L. Qin, *Adv. Sci.* **2020**, *7*, 201902443.
[49] a) L. C. Li, J. C. Gao, Y. Wang, *Surf. Coat. 80 [Eighty], Annu. Natl. Tech. Semin., 11th* **2004**, *185*, 92; b) R. C. Zeng, W. Dietzel, F. Witte, N. Hort, C. Blawert, *Adv. Eng. Mater.* **2008**, *10*, B3.
[50] A. M. Rashmirraven, D. C. Richardson, H. M. Aberman, D. J. Deyoung, *J Appl Biomater* **1995**, *6*, 237.
[51] D. W. Zhao, S. B. Huang, F. Q. Lu, B. J. Wang, L. Yang, L. Qin, K. Yang, Y. D. Li, W. R. Li, W. Wang, S. M. Tian, X. Z. Zhang, W. B. Gao, Z. P. Wang, Y. Zhang, X. H. Xie, J. L. Wang, J. L. Li, *Biomaterials* **2016**, *81*, 84.
[52] H. Q. Feng, G. M. Wang, W. H. Jin, X. M. Zhang, Y. F. Huang, A. Gao, H. Wu, G. S. Wu, P. K. Chu, *ACS Appl. Mater. Inter* **2016**, *8*, 9662.
[53] a) J. J. Deng, J. Ye, Y. L. Zhao, Y. L. Zhu, T. L. Wu, C. Zhang, L. N. Dong, H. Ouyang, X. G. Cheng, X. L. Wang, *ACS Biomater. Sci. Eng.* **2019**, *5*, 4285; b) M. K. Peng, F. Y. Hu, M. T. Du, B. J. Mai, S. R. Zheng, P. Liu, C. H. Wang, Y. S. Chen, *Front Mater. Sci.* **2020**, *14*, 14; c) H. Wu, K. Xi, S. Xiao, A. M. Qasim, R. K. Y. Fu, K. J. Shi, K. J. Ding, G. H. Chen, G. S. Wu, P. K. Chu, *Surf. Coat. Technol.* **2020**, *401*, 126251.
[54] V. Tsakiris, C. Tardei, F. M. Clicinschi, *J. Magnes. Alloy* **2021**, *9*, 1884.
[55] G. M. Wang, W. J. Jiang, S. Mo, L. X. Xie, Q. Liao, L. S. Hu, Q. D. Ruan, K. W. Tang, B. Mehrjou, M. T. Liu, L. P. Tong, H. Y. Wang, J. Zhuang, G. S. Wu, P. K. Chu, *Adv. Sci.* **2020**, *7*, 201902089.
[56] H. Y. Ma, A. X. Suonan, J. Y. Zhou, Q. L. Yuan, L. Liu, X. M. Zhao, X. X. Lou, C. C. Yang, D. C. Li, Y. G. Zhang, *Arab J Chem* **2021**, *14*, 102977.
[57] S. M. Kurtz, *PEEK Biomaterials Handbook* **2012**, 1.
[58] X. T. Han, D. Yang, C. C. Yang, S. Spintzyk, L. Scheideler, P. Li, D. C. Li, J. Geis-Gerstorfer, F. Rupp, *J Clin Med* **2019**, *8*, 240.
[59] S. Balachandran, Z. Zachariah, A. Fischer, D. Mayweg, M. A. Wimmer, D. Raabe, M. Herbig, *Adv. Sci.* **2020**, *7*, 1903008.
[60] S. M. Kurtz, J. N. Devine, *Biomaterials* **2007**, *28*, 4845.
[61] J. M. Toth, in *PEEK Biomaterials Handbook*, 2nd ed. (Ed: S. M. Kurtz), Elsevier, Amsterdam, The Netherlands **2019** Ch.8.
[62] *PEEK Biomaterials Handbook*, (Ed: S. M. Kurtz), Elsevier, Amsterdam, The Netherlands **2019**, 11.
[63] Z. Y. Chen, Y. Chen, J. D. Ding, L. Yu, *Compos. Part B-Eng* **2023**, *250*, 110427.
[64] L. P. Ouyang, Y. C. Zhao, G. D. Jin, T. Lu, J. H. Li, Y. Q. Qiao, C. Q. Ning, X. L. Zhang, P. K. Chu, X. Y. Liu, *Biomaterials* **2016**, *83*, 115.
[65] D. W. Chen, K. Y. Lee, M. H. Tsai, T. Y. Lin, C. H. Chen, K. W. Cheng, *Nanomaterials* **2019**, *9*, 713.
[66] J. Ye, J. J. Deng, Y. T. Chen, T. Yang, Y. L. Zhu, C. X. Wu, T. L. Wu, J. Y. Jia, X. G. Cheng, X. L. Wang, *Biomater. Sci.* **2019**, *7*, 2826.
[67] C. C. Liu, J. F. Bai, Y. Wang, L. Chen, D. F. Wang, S. L. Ni, H. Liu, *Dent Mater* **2021**, *37*, 81.
[68] X. Wang, T. Lu, J. Wen, L. Y. Xu, D. L. Zeng, Q. J. Wu, L. Y. Cao, S. X. Lin, X. Y. Liu, X. Q. Jiang, *Biomaterials* **2016**, *83*, 207.
[69] S. Mo, B. Mehrjou, K. W. Tang, H. Y. Wang, K. F. Huo, A. M. Qasim, G. M. Wang, P. K. Chu, *Chem. Eng. J.* **2020**, *392*, 123736.
[70] S. Mo, K. W. Tang, Q. Liao, L. X. Xie, Y. Z. Wu, G. M. Wang, Q. D. Ruan, A. Gao, Y. L. Lv, K. Y. Cai, L. P. Tong, Z. W. Wu, P. K. Chu, H. Y. Wang, *Mater. Horiz.* **2023**, *10*, 881.
[71] a) Y. Wu, P. Liu, Q. Liao, T. Jin, Z. Wu, G. Wang, H. Wang, P. K. Chu, *Adv. Healthcare Mater.* **2023**, 2302736; b) Y. Wu, Q. Ruan, C. Huang, Q. Liao, L. Liu, P. Liu, S. Mo, G. Wang, H. Wang, P. K. Chu, *Biomater Adv* **2022**, *134*, 112701; c) P. Liu, Y. Wu, B. Mehrjou, K. Tang, G. Wang, P. K. Chu, *Adv. Funct. Mater.* **2022**, *32*, 2110635; d) H. Xin, B. Li, L. Lee, *The Innovation Materials* **2023**, *1*, 100036.

[72] R. Kaur, S. Liu, *Prog. Surf. Sci.* **2016**, *91*, 136.
[73] M. J. Dalby, N. Gadegaard, R. O. C. Oreffo, *Nat. Mater.* **2014**, *13*, 558.
[74] D. A. Robinson, R. W. Griffith, D. Shechtman, R. B. Evans, M. G. Conzemius, *Acta Biomater.* **2010**, *6*, 1869.
[75] a) Y. H. Li, J. Wang, D. He, G. X. Zhu, G. Y. Wu, L. Chen, *J. Mater. Sci.: Mater. Med.* **2020**, *31*, 11; b) J. D. Burgal, L. G. Peeva, S. Kumbharkar, A. Livingston, *J. Membrane Sci.* **2015**, *479*, 105.
[76] J. Devaux, D. Delimoy, D. Daoust, R. Legras, J. P. Mercier, C. Strazielle, E. Nield, *Polymer* **1985**, *26*, 1994.
[77] Y. Zhang, J. S. Cui, K. Y. Chen, S. H. Kuo, J. Sharma, R. Bhatta, Z. Liu, A. Ellis-Mohr, F. F. An, J. H. Li, Q. Chen, K. D. Foss, H. Wang, Y. M. Li, A. M. McCoy, G. W. Lau, Q. Cao, *Sci. Adv.* **2023**, *9*, eadg7397.
[78] a) S. R. Oungoulian, K. M. Durney, B. K. Jones, C. S. Ahmad, C. T. Hung, G. A. Ateshian, *J. Biomech.* **2015**, *48*, 1957; b) N. E. Bishop, A. Hothan, M. M. Morlock, *J Orthop Res* **2013**, *31*, 807.
[79] S. B. Goodman, J. Gallo, E. Gibon, M. Takagi, *Expert Rev. Med. Devic.* **2020**, *17*, 41.
[80] L. X. Xie, G. M. Wang, Y. Z. Wu, Q. Liao, S. Mo, X. X. Ren, L. P. Tong, W. Zhang, M. Guan, H. B. Pan, P. K. Chu, H. Y. Wang, *The Innovation* **2021**, *2*, 100148.
[81] D. H. K. Nguyen, C. Loebbe, D. P. Linklater, X. M. Xu, N. Vrancken, T. Katkus, S. Juodkazis, S. Maclaughlin, V. Baulin, R. J. Crawford, E. P. Ivanova, *Nanoscale* **2019**, *11*, 16455.
[82] Z. T. Liu, Y. Z. Yi, L. J. Song, Y. X. Chen, L. M. Tian, J. Zhao, L. Q. Ren, *Acta Biomater.* **2022**, *141*, 198.

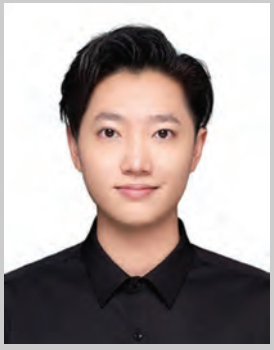

Yuzheng Wu studied physical chemistry and obtained his master's degree from the University of Chinese Academy of Sciences, China, in 2020. He joined the research group of Prof. Paul Chu at City University of Hong Kong in 2020 as a PhD student. His research interest is the modulation of bacterial behavior via materials interventions.

Pei Liu received her Ph.D. in physics from City University of Hong Kong in 2023 under the supervision of Prof. Paul K Chu. Her research focuses on the design of biomaterials and nanomaterials for interface construction for antibacterial applications.

Paul K Chu received his BS in mathematics from the Ohio State University and MS/Ph.D. in chemistry from Cornell University. He is chair professor of Materials Engineering holding joint appointments in the Department of Physics, Department of Materials Science & Engineering, and Department of Biomedical Engineering at City University of Hong Kong. His research interests are quite diverse encompassing plasma and materials science and engineering. In addition to being a fellow and council member of the Hong Kong Academy of Engineering Sciences, he is a fellow of the APS, AVS, IEEE, MRS, and HKIE. He is also a highly cited researcher.